A partially-coupled hydro-mechanical analysis of the Bengal Aquifer System under hydrological loading

Nicholas D. Woodman[1†], William G. Burgess[1], Kazi Matin Ahmed[2] and Anwar Zahid[3]

[1]Department of Earth Sciences, University College London, London WC1E 6BT, UK, [2]Department of Geology, Dhaka University, Dhaka 1000, Bangladesh, [3]Bangladesh Water Development Board, Dhaka, Bangladesh, [†]current address: Faculty of Engineering and the Environment, University of Southampton, Southampton SO17 1BJ, UK

Correspondence to: Nicholas D Woodman (n.d.woodman@soton.ac.uk)

Abstract. The coupled poro-mechanical behaviour of geologic-fluid systems is fundamental to numerous processes in structural geology, seismology and geotechnics but is frequently overlooked in hydrogeology. Substantial poro-mechanical influences on groundwater head have recently been highlighted in the Bengal Aquifer System, however, driven by terrestrial water loading across the Ganges-Brahmaputra-Meghna floodplains. Groundwater management in this strategically important fluvio-deltaic aquifer, the largest in south Asia, requires a coupled hydro-mechanical approach which acknowledges poro-elasticity. We present a simple partially-coupled, one-dimensional poro-elastic model of the Bengal Aquifer System, and explore the poro-mechanical responses of the aquifer to surface boundary conditions representing hydraulic head and mechanical load under three modes of terrestrial water variation. The characteristic responses, shown as amplitude and phase of hydraulic head in depth profile and of ground surface deflection, demonstrate (i) the limits to using water levels in piezometers to indicate groundwater recharge, as conventionally applied in groundwater resources management; (ii) the conditions under which piezometer water levels respond primarily to changes in the mass of terrestrial water storage, as applied in geological weighing lysimetry; (iii) the relationship of ground surface vertical deflection to changes in groundwater storage; and (iv) errors of attribution that could result from ignoring the poroelastic behaviour of the aquifer. These concepts are illustrated through application of the partially-coupled model to interpret multi-level piezometer data at two sites in southern Bangladesh. There is a need for further research into the coupled responses of the aquifer due to more complex forms of surface loading, particularly from rivers.

1 Introduction

Throughout the Bengal Basin, the floodplains of the Ganges, Brahmaputra and Meghna (GBM) rivers (Fig. 1) are underlain by the Bengal Aquifer System (BAS), the largest aquifer in south Asia and the source of water to over 100 million people (Burgess et al., 2010). More than 10 million tubewells throughout the basin provide water from BAS for domestic use and for

30   irrigation of the rice crop (Ravenscroft et al., 2009); these include hand-pumped tubewells, normally between 15 and 30 m

31   depth below ground level (bgl), for domestic use, and tubewells installed with motor-driven pumps to abstract water from

32   between 50 and 75 m depth bgl for irrigation of the dry season rice crop (January to April). Municipal water supplies commonly

33   abstract year-round from depths between 200 and 300 m bgl (Shamsudduha et al., 2018). Management of the BAS groundwater

34   resource relies on monitoring water levels in networks of observation boreholes, taking the conventional approach that changes

35   in groundwater heads represent volumetric changes in groundwater storage through recharge and drainage (Shamsudduha et

36   al., 2011). This approach presumes the hydraulic behaviour of the aquifer to be decoupled from its mechanical response to

37   changes in stress. Recently, however, the distinctively poroelastic behaviour of the BAS has been recognised (Burgess et al.,

38   2017), by which groundwater heads are subject to substantial mechanical perturbation driven by changes in the mass of

39   terrestrial water storage (TWS) above the surface of the aquifer. A coupled hydro-mechanical approach is necessary for

40   understanding groundwater conditions and managing resources in this environment, particularly in relation to recharge

41   (Shamsudduha et al., 2012), sustainability of groundwater abstraction for irrigation (Shamsudduha et al., 2008) and municipal

42   water supply (Ravenscroft et al., 2013), and the security of schemes for mitigation against groundwater arsenic (Michael and

43   Voss, 2008) and salinity (Rahman et al., 2011;Sultana et al., 2015).

44

45   The generally coupled poro-mechanical nature of geologic-fluid systems is well-established (Neuzil, 2003); porewater

46   pressures affect the stress state and vice-versa. These interactions are accepted as important where groundwater conditions are

47   related to faulting (Roeloffs, 1988;Rojstaczer and Agnew, 1989;Sutherland et al., 2017), earthquakes (Manga et al., 2012),

48   pumping-induced aquitard responses (Verruijt, 1969), ground subsidence (Burbey et al., 2006;Erban et al., 2014), glacial

49   loading effects (Bense and Person, 2008;Black and Barker, 2016) and surface water interactions (Acworth et al., 2015;Boutt,

50   2010). Use of ground surface vertical displacements to infer aquifer or groundwater conditions (Chaussard et al., 2014;Reeves

51   et al., 2014) is also predicated on coupling of the hydraulic and mechanical behaviour of aquifer sediments. For simulation of

52   transient groundwater flow in aquifers, however, a decoupling simplification is frequently applied such that the elastic equation

53   does not need to be solved simultaneously. Thus, the flow equation is solved without consideration of internal stresses and

54   strains or mechanical boundary conditions. Despite this, the poro-mechanical nature of confined aquifers is embedded in the

55   concept of specific storage which incorporates the elastic compressibility of the aquifer materials (Domenico and Schwartz,

56   1998;Green and Wang, 1990;Narasimhan, 2006). Furthermore, it is associated with the well known concept of barometric

57   efficiency (Spane, 2002), which describes the response of groundwater pressure to variations in atmospheric pressure, perhaps

58   the example of surface loading effects most familiar to hydrogeologists. The decoupling assumption is reasonable where the

59   effects of mechanical loading can be considered insignificant, either when the changes in load are small, or when the applied

60   load is mostly borne by the solid rather than the fluid (Black and Barker, 2016). Neither of these conditions apply to the BAS

61   sediments, which are highly compressible (Steckler et al., 2010) and subject to substantial and extensive TWS mechanical

62   loads due to heavy rainfall, deep flooding and large river discharges as a consequence of the annual monsoon (Shamsudduha

63   et al., 2012).

64

In the event of laterally-extensive changes to mechanical loads and/or hydraulic heads above the surface of an aquifer, and laterally-homogeneous aquifer properties, by symmetry it may be deduced that lateral strains are zero. This condition gives rise to a *partial* coupling of the elastic and fluid pressure equations (Neuzil, 2003). In the case of *partial* coupling, changes to the mechanical load due to the changing mass of water near or at the surface may be included within the flow equation, one-dimensionally in the vertical direction, and the solutions will satisfy all the equilibrium and compatibility requirements for stress and strain. There is no need to solve the elastic equation in order to calculate pressures in the aquifer, although once the flow equation is solved, the pressures can be substituted into the elastic equation to provide stresses and strains (Anochikwa et al., 2012). A sub-set of this partially-coupled condition occurs where there is negligible groundwater flow, due to very low hydraulic gradients, low permeability or a combination of both. This can be the situation in extensive fluvio-deltaic aquifers of low topographic relief such as the BAS (Burgess et al., 2017) if mechanical loading is imposed at the surface in a manner which does not induce significant vertical hydraulic gradients. Under these conditions, porewater pressures are determined by changes to surface mechanical loading alone, and changes in groundwater head may be taken as a measure of changes in TWS mechanical loading above the surface of the aquifer. This is the conceptual basis for geological weighing lysimetry (van der Kamp and Schmidt, 1997;Bardsley and Campbell, 1994, 2007;van der Kamp and Schmidt, 2017) as used in diverse environments to determine ΔTWS at the scale of individual catchments (Marin et al., 2010;Lambert et al., 2013;Barr et al., 2000;Smith et al., 2017). Geological weighing lysimetry has been suggested as suitable for mapping the variability of ΔTWS within the Bengal Basin (Burgess et al., 2017;Bardsley and Campbell, 2000), complementary to basin-scale estimates based on the Gravity and Climate Recovery Experiment (GRACE) satellite mission (Tapley et al., 2004;Tiwari et al., 2009;Shamsudduha et al., 2012).

84

The purpose of this paper is to explore the behaviour of the BAS as a poroelastic aquifer subject to a variety of extensive TWS mechanical and hydraulic loads. Poro-elastic theory is very well-established, but has not previously been applied in the context of a thick and extensive aquifer such as the BAS to show the implications for groundwater pressures together with solid strains and ground surface displacements.

89

The Bengal Basin has a tropical climate dominated by the Indian monsoon, with annual rainfall increasing from 1500 mm in the south and west to 5500 mm in north-east Bangladesh, of which 85% falls during the summer rainy season (May to November) when individual storm events can contribute over 100 mm per day (Ravenscroft, 2003). During the monsoon season, river levels rise by 2-8 m leading to widespread flooding (Steckler et al., 2010) with up to 30% of the land surface routinely being flooded to a depth up to ca. one metre. During the Boro rice irrigation season (January to April), groundwater pumping for irrigation throughout rural areas commonly provides standing water across rice paddies to a depth of ca 0.1 m (Hasanuzzaman, 2003). For the purpose of this paper, we treat the separate components of TWS across the GBM floodplains as *inundation* (free-standing surface water such as paddy, floods, beels, and ponds), *unconfined storage* (water in the

98 unsaturated zone and in saturated pores in the intermittently saturated zone of the aquifer), *elastic storage* (water in the

99 saturated pores in the permanently saturated zone), and *rivers* (surface water flowing in rivers and drainage channels).

100 Processes that alter the TWS loads include rainfall and evaporation, rising and falling river stage, flooding and drainage of the

101 land surface, varying soil moisture storage and a fluctuating water table. Groundwater pumping modifies the water balance

102 and induces additional hydro-mechanical responses. These processes differ in their timing, the geometry of the TWS stores

103 they affect and the relationship between their resultant hydraulic and mechanical expressions. First, we apply the concept of

104 *partial* coupling to seek characteristic responses of the aquifer to extensive TWS loads originating as (a) surface water

105 inundation, (b) water table fluctuation and (c) water bodies hydraulically isolated from the aquifer. These loading styles are

106 examined with and without pumping. The results address important questions for the BAS which are likely also relevant to

107 similarly extensive and strategically important fluvio-deltaic aquifer systems elsewhere in south Asia (Fendorf et al.,

108 2010;Benner et al., 2008;Larsen et al., 2008;Tam et al., 2014;Xu et al., 2011): how can piezometer heads in the poroelastic

109 aquifer be used to indicate recharge, as required for conventional groundwater resources management; under what conditions

110 can piezometer heads be used to measure ΔTWS using geological weighing lysmetry; can ground surface deflections be related

111 to changes in groundwater storage; and what errors may arise if the poroelastic behaviour of the aquifer is ignored? Second,

112 we apply the partial coupling approach to these questions in the BAS, with reference to multi-level piezometer data from

113 Khulna and Laksmipur in southern Bangladesh (Fig. 1).

114 **2 Methods**

115 We firstly set out the partially-coupled 1D poromechanical approach that we use to examine the implications of specific surface

116 (upper boundary) loading scenarios, with aquifer parameters set to represent the BAS underlying the GBM floodplains (Fig.

117 1). We consider an equivalent homogeneous uniform medium, as well as a layered structure based on lithological sections.

118 The results provide a diagnostic framework which we apply to analysis of loading styles at Khulna and Laksmipur in southern

119 Bangladesh.

120
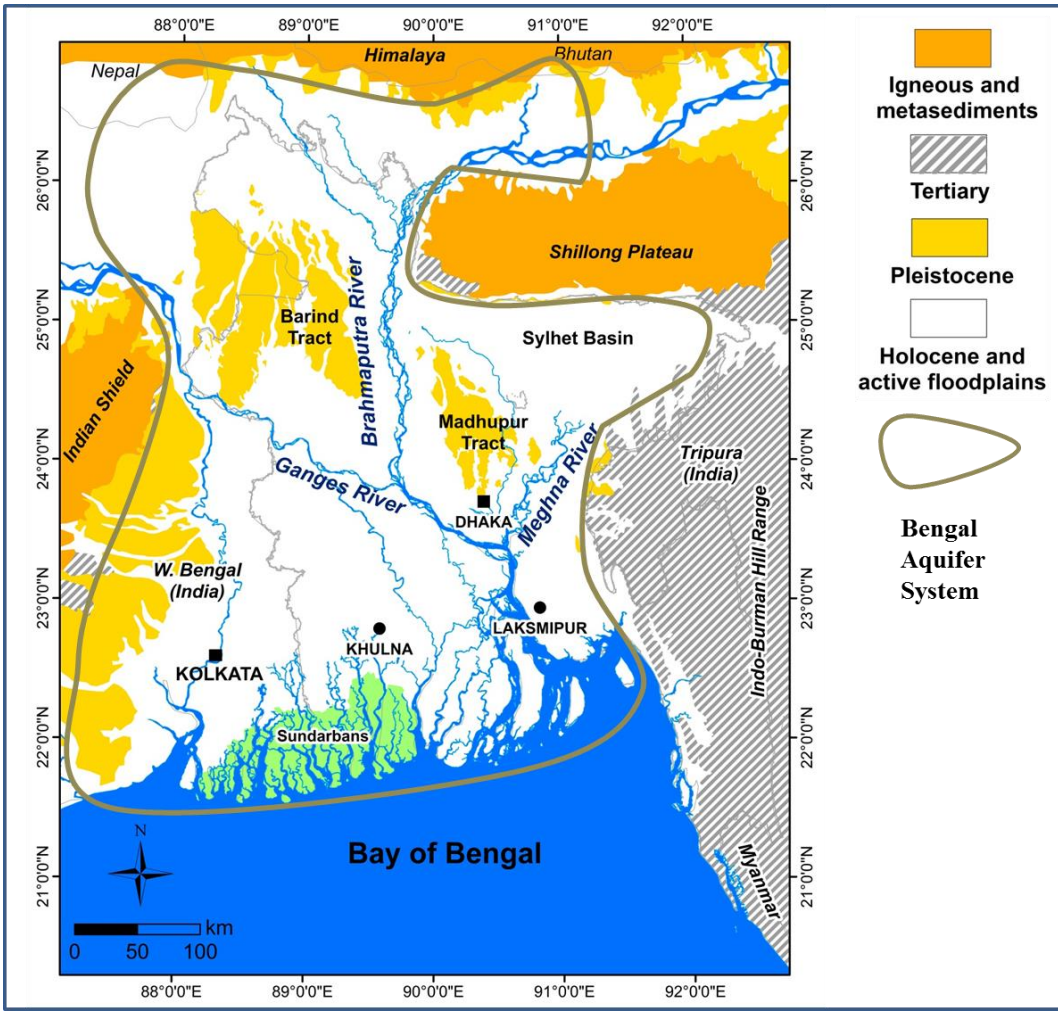
Figure 1. Location map showing the extent of the Bengal Aquifer System (BAS) and the Ganges-Brahmaputra-Meghna (GBM) floodplains.

2.1 Poromechanical equations

We concentrate on the coupling between water flow and the mechanical behaviour of the BAS sediment, assuming isothermal conditions and that the aquifer material behaves in a linear-elastic way. This is likely to be reasonable under repeated mechanical load-unload cycles, provided there is no secular decline in groundwater level sufficient to cause effective stress to exceed the previous loading maximum.

The 3D flow and mechanical equations are given in the Appendix. In the event of uniform (1D) areal mechanical loading, and where lateral strains are negligible, the system simplifies to a flow equation coupled to a mechanical equation for 1D loading:

$$\nabla \cdot \kappa(\nabla p + \rho g \nabla z) = S_s \frac{\partial p}{\partial t} - S_s \xi \frac{\partial \sigma_{zz}}{\partial t} - gJ \tag{1}$$

131   where κ is the hydraulic conductivity (m s^{-1}), ρ is the fluid density (kg m^{-3}), p is the pore pressure (Pa), z is the elevation (m),

132   J (kg m^{-3}d^{-1}) is a fluid source term used here to simulate groundwater abstraction by pumping, ξ is the one-dimensional loading

133   efficiency (given in Appendix A5), ν is Poisson's ratio (-), S_s is the one-dimensional specific storage typically used in

134   groundwater analyses (van der Kamp and Gale, 1983).

135

136   The sediment is assumed to sit on a rigid base, with the top surface free to move, so strain can only be vertical. Thus from

137   Equation A1, the vertical stress and strains are related by:

$$\sigma_{zz} = K'\varepsilon_{zz} + \alpha_B p \qquad\qquad (2)$$

138   where $K' = 3K(1-\nu)/(1+\nu)$, α_B is the Biot-Willis coefficient (assumed equal to 1 to simulate incompressible particle

139   grains) and the bulk modulus, K and shear modulus, G are related to Young's modulus E by $K = \frac{E}{3(1-2\nu)}$ and $G = \frac{E}{2(1+\nu)}$.

140   Changes to the total vertical stress, σ_{zz} (here termed 'mechanical loads') are applied as a boundary condition at the surface,

141   and are transmitted by the solid skeleton to the entire solid at the acoustic velocity. This represents 'partial coupling'; if there

142   are negligible internal loads and provided the changes to the surface load are known, then the flow equation (1) can be solved

143   without a need to solve the elastic equations. Deformations can be found from Eq. (2), in conjunction with the compatibility

144   relationships.

145

146   The simplified system considered here is given in Fig. 2. On the upper boundary, the changing TWS is simulated by means of

147   a changing head and a changing mechanical load, according to the nature of the contributing hydrological components. Under

148   this simplification, vertical displacement at the surface will arise in only two ways: by contraction or expansion of the pore

149   space where there is a net change in the volume of water in the column, and by contraction or expansion of the pore water.

150   Being limited to 1D movement, these volume changes are entirely taken up by vertical displacement.

151

152   The reference frame is the base of the model which is assumed fixed in space and set at 1 km depth, acknowledging the

153   variation in aquifer thickness between south-east Bangladesh, 3000 m (Michael and Voss, 2009a) and West Bengal, 300 m

154   (Mukherjee et al., 2007). Within this domain, equations (1) & (2) are solved analytically for a homogeneous uniform material

155   in the absence of pumping, and numerically where layers of individually homogeneous materials are simulated, with and

156   without pumping. Where pumping is simulated, the water is assumed to be taken uniformly from the pumping-interval. For

157   simplicity, earth-tides are neglected.

158

2.2 Analytical solution

Taking Eq. (1) and assuming homogeneous K, E and that $J = 0$, converting p to metres head, h (i.e. $h = \rho g p + z$), and σ_{zz} to metres of load (i.e. $L = \sigma_t/\rho g$, where ρ (kg m^{-3}) is the density of water and g (m s^{-2}) is the acceleration due to gravity) (Anochikwa et al., 2012;van der Kamp and Schmidt, 1997) gives:

$$D\frac{\partial^2 h}{\partial z^2} = \frac{\partial h}{\partial t} - \xi\frac{\partial L}{\partial t} \tag{3}$$

where 1D hydraulic diffusivity is defined as $D = \frac{k}{S_s}$.

Applying the following sinusoidal hydraulic and mechanical loading boundary conditions to Eq. (9) where we introduce parameter, α, which can be set to zero to give the case of a load in the absence of a varying head, and otherwise is kept at 1:

$$h(0,t) = H(t) = \alpha H_0 \cos(\omega t) \tag{4}$$
$$L(t) = S_y H_0 \cos(\omega t)$$

The following solution is obtained:

$$h(z,t) = \alpha B \cos(\omega t - \psi) \tag{5}$$

where ψ is the lag (in radians) behind the head $H(t)$ and mechanical loads $L(t)$ at the boundary and:

$$B = \sqrt{\gamma^2 + 2\gamma(\alpha - \gamma)e^{-\theta}\cos(\theta) + (\alpha - \gamma)^2 e^{-2\theta}} \tag{6}$$

$$\psi = \tan^{-1}\left(\frac{(\alpha - \gamma)\sin(\theta)}{(\alpha - \gamma)\cos(\theta) + \gamma e^{\theta}}\right)$$

$$\theta = z\sqrt{\frac{\omega}{2D}} = z\sqrt{\frac{\pi}{DT}} \quad \text{and} \quad \gamma = S_y\xi$$

In the event that the mechanical load, L, is negligible compared to applied head H (e.g. where either S_y is very small or ξ is very small), the hydraulic-only solution is well known (van der Kamp and Maathuis, 1991):

$$h(z,t) = H_0 \exp(-\psi)\cos(\omega t - \psi) \tag{7}$$

where the lag is now $\psi = \theta$. Thus, the lag increases with depth or with increasing forcing frequency and the amplitude decreases exponentially with θ.

Displacement and change in groundwater storage can be calculated as the time integral of velocity at the surface. Applying Darcy's law at the surface (z=0) and integrating gives:

$$u = \Delta S = \int_0^t K\frac{dh}{dz}\bigg|_{z=0} dt' \tag{8}$$

Equation (8) can be computed by differentiating Eq. (5) w.r.t. z and then numerically integrating over time. Alternatively, the change of storage can be reported from the numerical model.

2.3 Numerical solution

We used the COMSOL Multiphysics® software, validated against the analytical solutions for uniform permeability, to solve the stress and flow equations (1) and (2). The finite-element model is unrestricted in terms of spatial distribution of parameter properties and in terms of the boundary condition functions.

2.4 Parameter allocation

Selected parameter values for the BAS underlying the GBM floodplains are given in Fig. 2. The bulk values for the uniform representations are close to the harmonic average of the series components. We next discuss the context in which these parameter selections are made.

2.4.1 Modulus of elasticity, storativity and loading efficiency

Text-book S_s values (Domenico and Schwartz, 1998) for the materials in the Bengal Basin range between approximately 1×10^{-5} m^{-1} (dense sandy gravel) and 1×10^{-2} m^{-1} (plastic clay). In large-scale modelling of head recession data in the basin Michael & Voss (Michael and Voss, 2009b) achieved their best fits when S_s was 9.4×10^{-5} m^{-1} taking pumped abstraction to be areally uniform. This is the basis for the range in specific storage, S_s, for the BAS (Fig. 2).

192
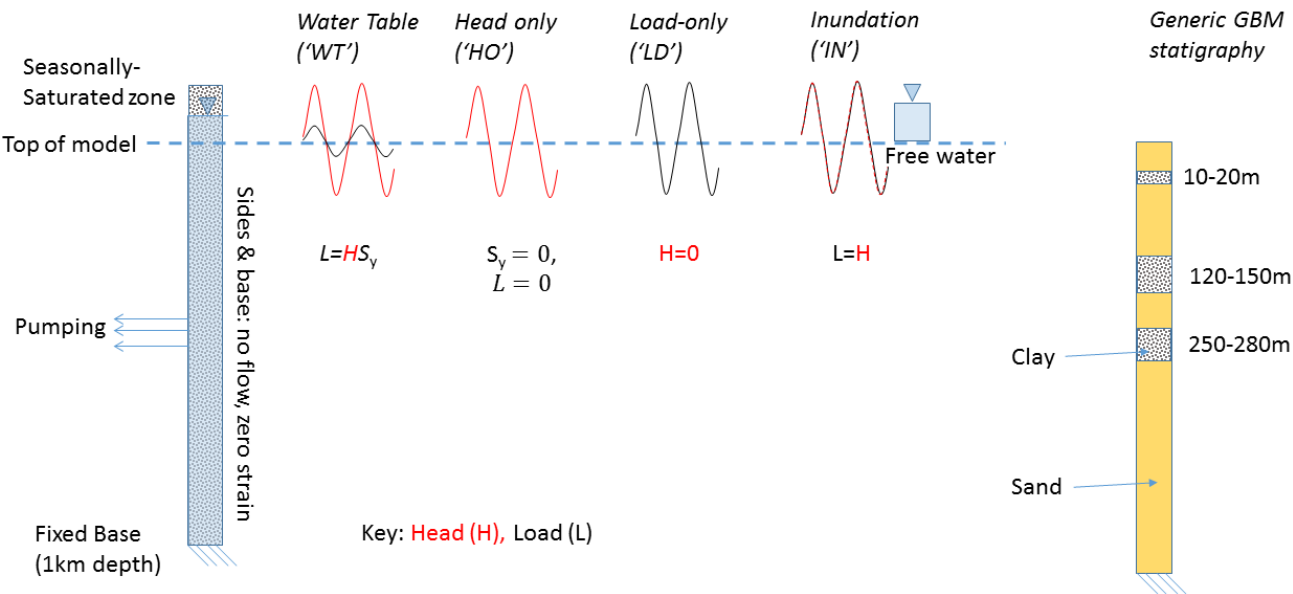
	Uniform	Layered representation						
			2 (silty-		*4 (silty-*		*6 (silty-*	*7*
	homogeneous	*1 (sand)*	*clay)*	*3 (sand)*	*clay)*	*5 (sand)*	*clay)*	*(sand)*
Thickness (m)	1000	10	10	100	30	100	30	720
S_y (-)	0.1 [1]	0.1	-	-	-	-	-	-
S_s (m^{-1})	0.00001 [2]	1×10^{-5}	1×10^{-4}	1×10^{-5}	1×10^{-4}	1×10^{-5}	1×10^{-4}	1×10^{-5}
K_v (ms^{-1})	0.00000005 [3]	1×10^{-5}	1×10^{-8}	1×10^{-5}	1×10^{-8}	1×10^{-5}	1×10^{-8}	1×10^{-5}
E (MPa)	82.07	850.89	82.07	850.89	82.07	850.89	82.07	850.89
ξ (-)	0.993	0.932	0.993	0.932	0.993	0.932	0.993	0.932

193

Figure 2. The 1D model showing (top) the upper surface boundary conditions with head as red lines and mechanical load (weight) as black lines, expressed as metres of water; and a representative stratigraphy for the BAS underlying the GBM floodplains, with the profile depth being 1 km; and (bottom) parameter values for the uniform and layered 1D representations. Porosity is taken as 0.1 throughout; ν=0.25; E, and ξ are calculated using Equations (A3, A4 and A5). [1] (Shamsudduha et al., 2011); [2] (Burgess et al., 2017); [3] (Michael and Voss, 2009a).

199

200 Specific storage S_s and Young's Modulus E are related though Eq. [A3] and to the loading efficiency ξ via Eq. (A4). These

201 inter-relationships are plotted in Fig. 3. It is notable that for $E<1$ GPa, $\xi>0.95$ and $S_s>1\times10^{-5}$ m^{-1}. Thus the loading efficiency

202 only falls significantly below 1 for materials stiffer than around 1 GPa, and where the specific storage is less than 1×10^{-5} m^{-1}.

203 Uncemented sediment is thus expected to have $\xi\sim1$ (Bakker, 2016); on this basis the BAS sediment is unlikely to be sufficiently

204 stiff in the top few hundred metres to allow decoupling of the stress and flow equations. This is corroborated by in situ, high-

205 pressure dilatometer measurements(de Silva et al., 2010) giving E within the broad range for sediments given in Fig. 3.

206
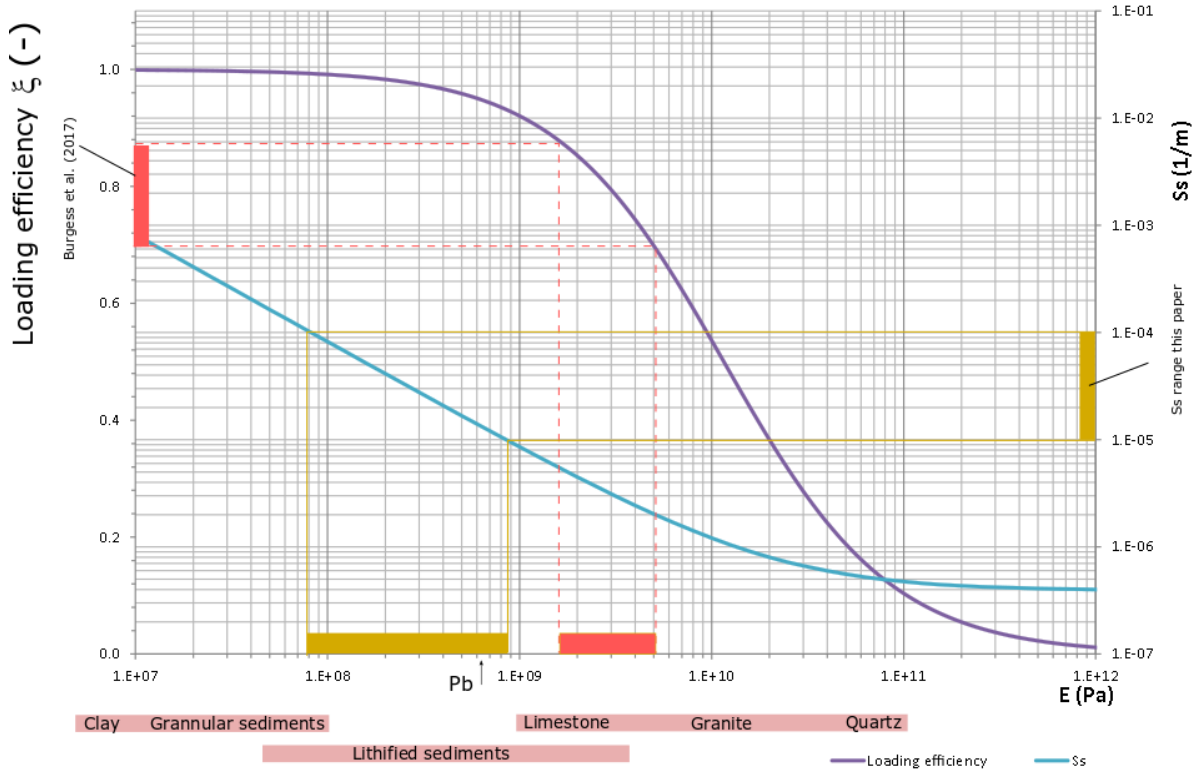
207 **Figure 3. Relationship between 1D Specific storage (S_s), Young's modulus (E) and 1D loading efficiency (ξ) using equations (A3, A4**
208 **and A5) assuming porosity of 0.1 and Poisson's ratio of 0.25. Projections show the corresponding inferred ranges of E based on the**
209 **S_s range applied (1×10^{-5} - 1×10^{-4} m^{-1}) and the loading efficiencies calculated via barometric efficiency estimates (0.69-0.87) by Burgess**
210 **et al. 2017. Pink bars show indicative ranges for common geological materials. Arrow indicates data from 73 m depth at Padma**
211 **Bridge (Pb) (De Silva *et al.*, 2010).**

212 Estimates of (1D) loading efficiency based (Jacob, 1940) on barometric efficiency are rather lower: a range of 0.69-0.87 has

213 been determined at Laksmipur in the GBM sediment (Burgess et al., 2017). This is potentially indicative of a considerable

214 stiffening due to burial (E in the range 6-17 GPa), indicating S_s in the range 1×10^{-6} to 9×10^{-8} m^{-1}. Such a condition might be

215 expected in a Gibson soil (Gibson, 1974;Powrie, 2014). However, the Laksmipur estimates do not decrease systematically

216 with depth, possibly due to changes in stiffness in different materials. The discrepancy may alternatively be related to the

217 timescale of processes responsible for changes in groundwater pressure. Barometric efficiency measurements operationally

218 consider short-term pore pressure changes likely corresponding to the response of relatively stiff aquifer sands, whereas

219 pressure changes in clays are expected to become significant in the longer term. Where short-term moisture loading effects are

220 the key interest (Anochikwa et al., 2012;Bardsley and Campbell, 2000), values for loading efficiency derived from barometric

221 efficiency may be the most appropriate. Here however our main concern is for poromechanical consistency and for water load

222 changes operating over a range of time scales, therefore we adopt S_s estimates based on aquifer pumping tests and use the

223 corresponding ξ and E values (Figure 3).

2.4.2 Hydraulic conductivity

225 Basin scale modelling suggests a horizontal-vertical anisotropy for hydraulic conductivity in the BAS of ~10,000 (Michael

226 and Voss, 2009b;Ravenscroft et al., 2005). This may be explained as an effective, large-scale value incorporating finer-scale

227 detail of the highly heterogeneous sedimentary record of the past deltaic environment where low permeability lenses and

228 drapes are laterally discontinuous (Hoque et al., 2017). Michael and Voss (Michael and Voss, 2009a) cite aquifer tests (Hussain

229 and Abdullah, 2001) conducted by the Bangladesh Water Development Board (BWDB) giving a range for hydraulic

230 conductivity (κ) from 3×10^{-5} to 1×10^{-3} m s^{-1}. Accounting for anisotropy, κ_v may therefore locally be in the range $\sim1\times10^{-9}$ to

231 1×10^{-7} m s^{-1}. The κ_v values of the uniform and layered representations of the BAS underlying the GBM floodplains (Fig. 2)

232 and of silty-clay in layered representations of the Khulna and Laksmipur sites (Sect. 4) lie within this range.

2.4.3 Specific yield

234 Specific yield is the drainable porosity of the material in which the water table moves. Michaels and Voss (Michael and Voss,

235 2009b) cite a range from 0.02 to 0.19 in Bangladesh, noting that much of the Basin has a specific yield in the range of 0.02–

236 0.05. We take S_y=0.1 and 0.01 as order-of-magnitude values typical for sand and clay respectively (Domenico and Schwartz,

237 1998).

2.5 Upper boundary conditions and groundwater abstraction

239 Changes to the shallow water budget which have the potential to be laterally-extensive and uniform include: water arriving as

240 rainfall at the surface and either ponding or moving to the shallow water table as recharge; and water departing the surface or

241 the water table by evaporation, or as runoff to the extensive network of drainage channels. Pumping for domestic and irrigation

242 supply may potentially be considered as areally-uniform, where sufficiently common and over a wide area (Michael and Voss,

243 2008). The changing shallow water budget causes a change in mechanical loading to the aquifer system, and if in direct

244 hydraulic continuity with the saturated water column it also causes a change in head. If the shallow water is not hydraulically

245 connected to the saturated aquifer system, the effects of the changing water budget are transmitted to depth by mechanical

246 compression/extension of the sediment, but not by hydraulic diffusion. Changes to the barometric pressure also apply a

247 laterally-extensive changing force to the surface of the aquifer and to the water column, and earth tides are also laterally-

248 extensive. The daily perturbation on water heads by atmospheric pressure changes is of the order of 0.01m (Burgess et al.,

249 2017), which is small compared to the annual hydrograph amplitude of the order of 1 m. Barometric pressure and earth tides

250 are both neglected for simplicity here.

251

252 To explore the consequences of these hydraulic and mechanical loading sources, the groundwater dynamics associated with

253 three upper surface boundary conditions are modelled here (Fig. 2). Firstly, the effect of a changing level of free water is

254 examined, such as would be seen in paddy-fields, ponds or during floodwater inundation. This condition is here termed 'IN'.

255 The change in free-water level is equal to both the change in head and the change in mechanical load at the upper surface (load

256 is here parameterised in metres of water rather than as a stress). Secondly, the effect of changes to unconfined storage due to

257 a moving water table is examined. This condition is here termed 'WT'. The change in load is the specific yield times the head.

258 For very small specific yields this condition approaches the hydraulic-only ('HO') loading case, whereby there is insignificant

259 mechanical load, despite the change in head. Thirdly, we examine the effect of a changing surface water store (which could be

260 either free water held above an impermeable barrier, or a perched phreatic aquifer) which is hydraulically isolated from the

261 main aquifer system. A mechanical load only is applied, therefore no head change is applied to the aquifer and this condition

262 is termed 'LD'.

263

264 These three TWS loading scenarios are applied in turn to a uniform and a layered representation of the BAS underlying the

265 GBM floodplains. The loading is applied as sinusoidal functions with unit amplitude and time period of 1 year to simulate the

266 annual hydrological cycle. Additionally, the effects of groundwater abstraction are simulated. Abstraction is taken evenly from

267 the depth interval 50-100 m at an average rate of 0.2 m a^{-1}, either as continuous pumping or as discontinuous pumping π out

268 of phase with the TWS load, as a coarse representation of seasonally-varying pumping for irrigation during the dry season.

269

270 3 Forward modelling results

271 The modelled responses of groundwater head to sinusoidal hydraulic and mechanical source terms, together with changes in

272 groundwater storage and ground surface vertical displacements, are illustrated for the GBM environment with uniform

273 properties in Figures 4 and 5. Figure 4 shows the modelled responses over ten years at depths of 30, 100 and 300 m,

274 approximating typical BWDB multi-level piezometers (BWDB, 2013). The depth variations of amplitude and phase for

275 groundwater head and the phase-lag for surface displacement are summarised in Fig. 5. The effect of layering (Supporting

276 Information) is to cause departure from the uniform cases, so interpretation of data in a real, heterogeneous aquifer should take

277 into account local deviation from idealised uniform conditions. However, in general, the loading style ('IN', 'WT', 'LD') and

278 pumping regime are of more significance for the head responses and surface displacements than the detail of the BAS
279 stratigraphy.

3.1 The free surface water inundation scenario ('IN')

281 Under free-surface water inundation, head changes are characteristically equal in amplitude at all depths and in-phase with the
282 inundation signal. Away from the top boundary, the instantaneous head due to loading in this case is $h = \xi L$. Since ξ is close
283 to 1 and $H = L$, the head is everywhere almost equal to the mechanical load given that at the top boundary the head is also
284 $h = H$. Therefore under free-surface water inundation in the absence of pumping, piezometers at all depths can be expected to
285 record the surface water mechanical load, effectively operating as weighing lysimeters. The vertical displacement of the ground
286 surface is extremely small (amplitude ~0.4 mm), being due to the small compression of porewater itself over the 1 km
287 simulated depth, and is out of phase with the load (i.e. the ground surface moves downwards under an increasing load). The
288 amplitude of change in saturated storage is infinitesimal (~0.02 mm). The system is essentially 'un-drained'; water does not
289 flow in or out of the pores which therefore experience only minimal strain.
290

Scenario	Head (m)	Storage (dashed line) and displacement (solid line) (m)
(a) 'IN'		
(b) 'WT' S_y=0.1		
(c) 'WT' S_y=0.01		
(d) 'LD'		
(e) 'IN' Const. Q		
(f) 'IN' Cyclic Q.		
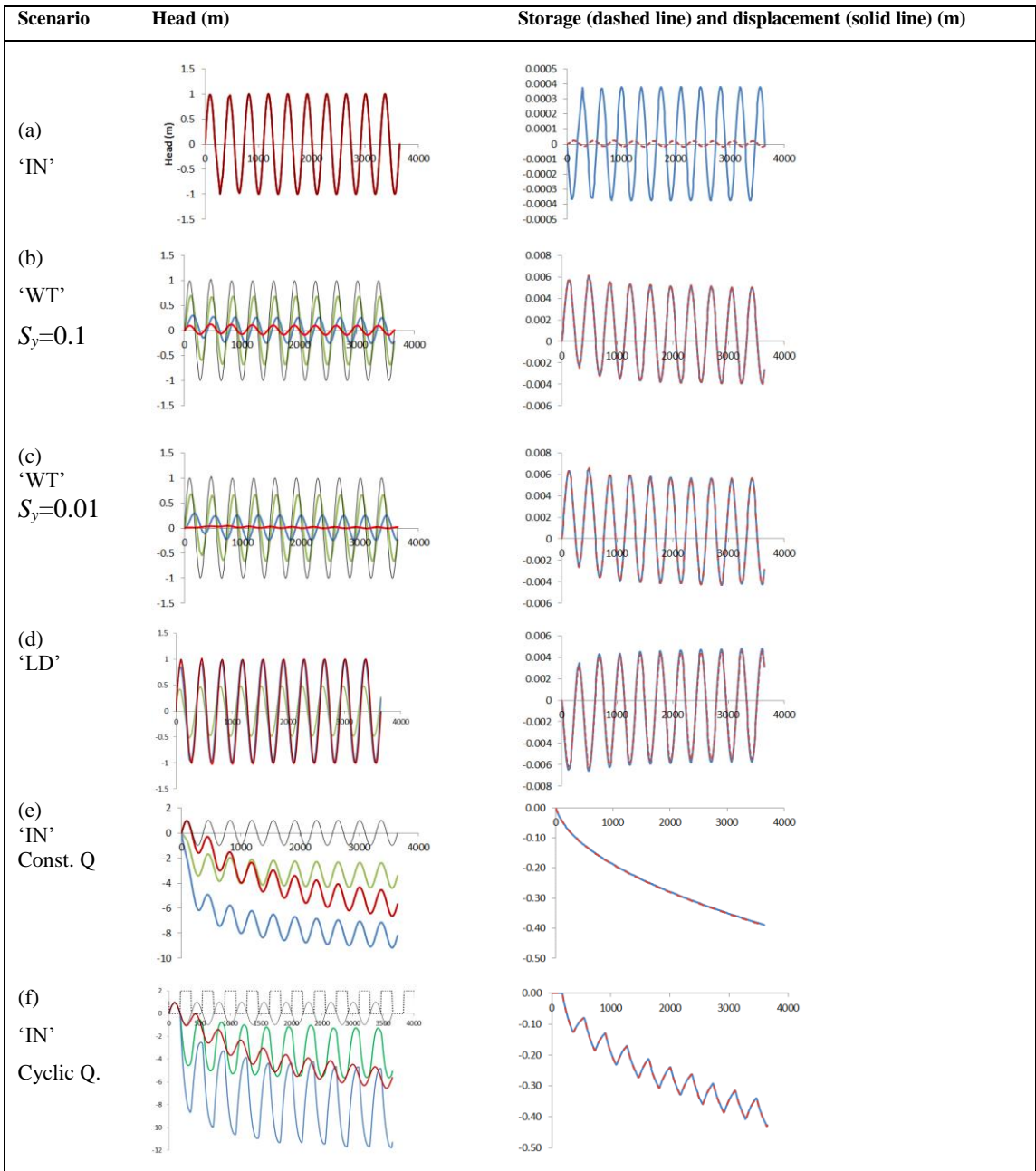
Figure 4. 1D model simulations for the GBM environment, showing results for the scenarios (a) 'IN', (b) 'WT' (S_y=0.1), (c) 'WT' (S_y=0.01), (d) 'LD', (e) 'IN' with constant pumping, (f) 'IN' with cyclic pumping, (see text for explanation). The x-axis is time in days, shown to 10 years (i.e. 3650 days). The amplitudes reported in the text are calculated from the max-min of the last annual cycle. Left: The y-axis is head, in metres (m). The surface head and/or mechanical load boundary conditions (black line) are expressed as equivalent m head (for the WT condition the unit variation of head is given and the S_y variation in mechanical load is not shown); results are in green (30 m depth), blue (100 m depth) and red (300 m depth) in all cases. For (a) results are co-linear at all depths; for (f) the intermittent pumping is shown as off/on by the square-wave dotted line. Right: The y-axis has dimension of length, in metres (m), showing changes in storage (dashed red line) and surface displacement (solid blue line) for each scenario.
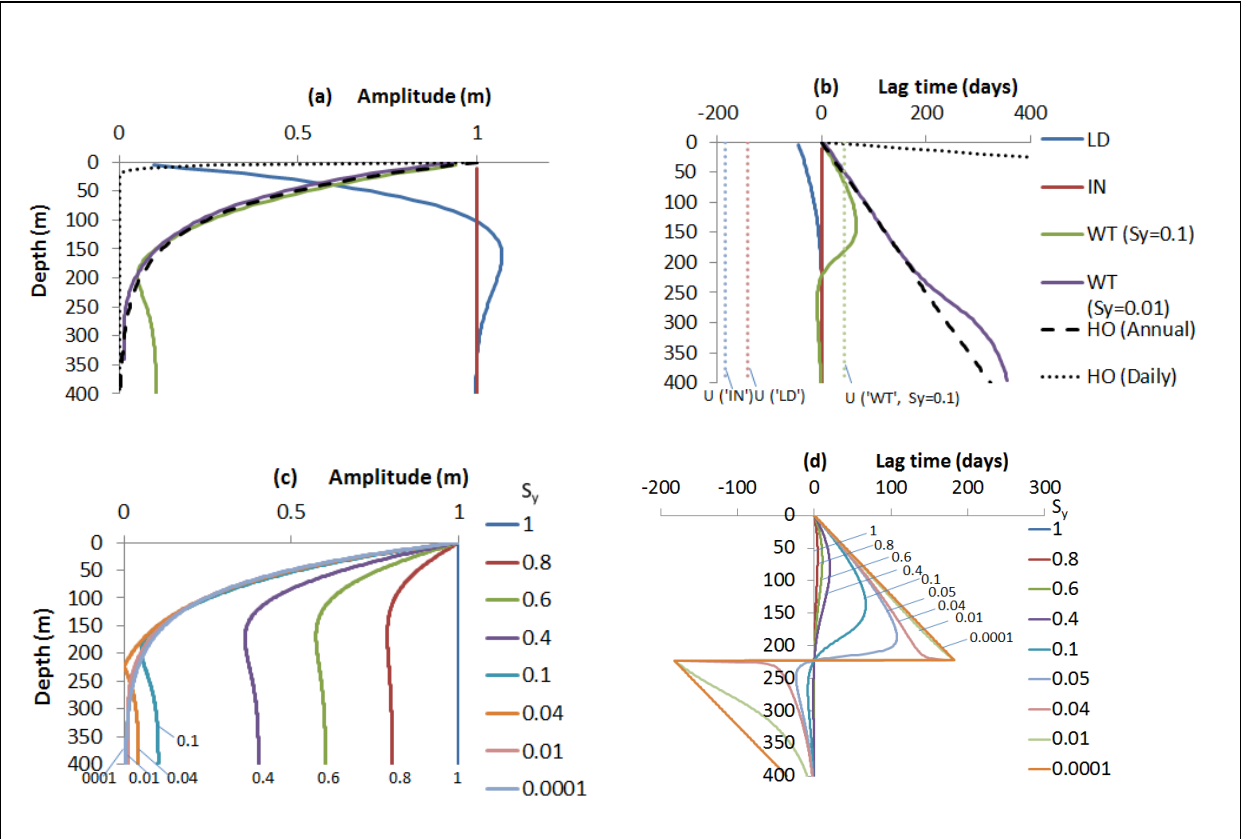
Figure 5. Profiles with depth for (a) amplitude of head response, (b) phase of head response and surface displacement (U), (c) sensitivity of amplitude to S_y for the 'WT' boundary condition, (d) sensitivity of phase to S_y for the 'WT' boundary condition. For (a) and (b) the colour code for the scenarios 'LD', 'IN', 'WT' (S_y=0.1), 'WT' (S_y=0.01), and HO, is shown in the top right panel (see text for explanation); in (b), displacement for the WT, S_y=0.01 scenario overlies that for the WT, S_y=0.1 scenario, so is not shown. (Note, in the instance that ξ is not close to 1, S_y in these plots can be substituted by $\gamma = S_y\xi$)

3.2 The variable water table scenario ('WT')

By contrast with the 'IN' scenario, head changes determined by a moving water table are depth-variable in amplitude and phase. When $S_y \rightarrow 0$ the 'WT' condition tends to the head-only end-member ('HO') and when $S_y \rightarrow 1$ the 'WT' condition tends to the 'IN' scenario. The maximum lag for $S_y = 0.1$ is at 137 m depth (or $\theta = 1.94$), beyond which it reduces (Fig. 5b). The sensitivity in head to S_y for the 'WT' scenario is illustrated in Fig. 5c. The amplitude of head responses is less than the water table fluctuation at all depths. Moreover, only a deep piezometer such as the one indicated at 300 m (Fig. 4b) will behave as a weighing lysimeter in this scenario. Here, heads are in phase with the water table and have approximate magnitude, $h = \xi L = \xi S_y H$, as in the study by van der Kamp and Maathuis (van der Kamp and Maathuis, 1991) of a thick aquitard overlying a confined aquifer. At 100 m the amplitude of head change is greater than at 300 m, and lags behind the water table. At 30 m the amplitude of head change is greatest and the lag is less than at 100 m. The difference in the head responses compared to

315 the 'IN' scenario is due to the difference in magnitudes of the applied head and applied load under the 'WT' scenario, causing

316 an instantaneous internal head gradient which subsequently diffuses. Ground surface displacement is ~4 mm and lags the load

317 by 44 days. With increased head at the top boundary, the upper surface moves upwards because as higher heads penetrate the

318 aquifer the effective stress is reduced. The lag is due to the time taken for the surface head to diffuse downwards.

3.3 The hydraulically disconnected load scenario ('LD')

320 Heads in the case of a surface load hydraulically isolated from the aquifer show a third characteristic behaviour. In this case

321 the amplitude of head change increases from zero at the top boundary (Fig. 5a), reaching a peak which is greater than the load,

322 1.07 m at 162 m (or θ =2.29). The amplitude thereafter tends to ξL at greater depth, whist the lag tends to zero. Therefore

323 heads in relatively deep piezometers potentially represent the surface load under a 'LD' boundary condition, as in Fig. 4d

324 where the heads at 300 m match the surface load, whereas at 30 m they do not. This is due to upward head diffusion towards

325 the surface where the head boundary condition is h=0. The lag which occurs in the 'WT' scenario due to the applied head

326 exceeding the mechanical load is reversed in this 'LD' scenario, becoming a lead time as the applied load exceeds the applied

327 head. Surface displacement is out of phase with the load, leading by ~π radians. The ground surface displacement amplitude

328 of ~4 mm is ten times greater than for the 'IN' scenario but is still very small in comparison to the annual variability of order

329 10 cm measured by GPS (Steckler et al., 2010). The 'LD' behaviour can be interpreted by means of a decomposition of heads

330 in the manner shown by Anochikwa et al. (Anochikwa et al., 2012) (see Supporting Information).

3.4 The influence of pumping

332 Introduction of pumping from the depth interval 50-100 m causes hydraulic dis-equilibrium which continues well beyond the

333 ten years' simulation, as the head drawdown propagates deep into the profile. As well as drawing water from storage at depth,

334 pumping induces recharge from the surface, there being a downward hydraulic gradient from the surface to the pumped

335 horizon, and upwards from the deeper levels to the pumped horizon. Variable perturbation due to the 'IN' surface load is

336 nevertheless clearly evident in the deep groundwater head measurements following correction for secular decline (Fig. 4e).

337 Elastic displacement, manifested as ground surface decline, exceeds 40 cm after ten years of pumping but, as in the un-pumped

338 'IN' scenario, the annual fluctuation due to surface loading is vanishingly small (0.03 mm). Thus, in addition to the possibility

339 of irreversible plastic deformation, elastic strain may gradually increase due to continuous pumping as stored water is drawn

340 from increasing depths.

341

342 Intermittent pumping strongly increases the seasonal variation in heads at the depth of pumping and this disturbance diffuses

343 to adjacent levels. However, as in the case of continuous pumping, the surface load signal is largely preserved in the deep

344 groundwater head response at 300 m. Also, intermittent pumping induces the same average long-term secular decline in stored

345 water volume and ground surface displacement as continuous pumping, but with additional annual fluctuation caused by the

346 pump switching on and off (decline/drawdown during the dry period when the pumps are used for irrigation and recovery
347 during the rainy season when the pumps are off).

348 **3.5 Model results for ground surface displacement**

349 Taking into account a small correction for the compressibility of water, surface displacement in the model is almost equal to
350 the total change in elastic storage in the permanently saturated aquifer. For the cases where pumping dominates the removal
351 of water, surface displacement is in phase with the pumping (Fig. 4f). For the cases which set up a diffusion of the hydraulic
352 signal between the surface boundary and the aquifer, the phase of surface displacement depends on the hydraulic (non-loading)
353 head changes at all depths (Fig. 4b, c, d). Therefore the lag for vertical displacements under the 'LD' surface condition is $\sim\pi$
354 out of phase with displacement under the 'WT' condition. Note from Eq. [6] that the amplitude and lag are both a function of
355 $\theta = z\sqrt{\dfrac{\omega}{2D}} = z\sqrt{\dfrac{\pi}{DT}}$ and therefore the solutions given here would be scaled in z by any changes to bulk diffusivity, D, and signal
356 frequency (or time period, T): higher frequency would give the same distribution but for a smaller z and the reverse would be
357 true for diffusivity. Intermittent pumping produces the largest cyclic displacements, however, in the order of centimetres,
358 because this condition causes the greatest volume of seasonal drainage from the formation itself. Where there is non-uniform
359 loading, as produced for example by a variable river stage, lateral groundwater drainage may occur and surface vertical
360 displacements may be greater under these conditions too.
361

362 **4 Applying the partial coupling analysis to field data**

363 Applying the 1D partial-coupling analysis to field data, we examine poromechanical perturbations at two sites, Khulna and
364 Laksmipur in southern Bangladesh (Fig. 1). Hourly measurements of groundwater pressure made between April 2013 and June
365 2014 in three closely-spaced piezometers between 60 and 275 m depth at each site are illustrated as hydrographs of equivalent
366 freshwater head in Supporting Information. Data on changes of the actual water table at the field sites are unfortunately not
367 available.
368 The objective here is to apply the principles and assumptions of the partially-coupled hydro-mechanical approach to reproduce
369 the characteristic features of the multi-level groundwater hydrographs using broadly representative aquifer parameters, rather
370 than to attempt an exact match by inverse modelling. Inspection of the hydrographs at both sites indicates, by reference to
371 Figures 4 and 5, that mechanical loading significantly influences the measured heads. Additionally, the presence of thick clay
372 aquitards at both sites (Figures 6, 7) suggests conditions under which heads may be determined solely by mechanical loads
373 and piezometers might behave as geological weighing lysimeters; a possibility which we put to the test.
374

375 The approach at each site is as follows:

376   i. A two-component sand-clay stratigraphy is based on site data, and parameter values are selected from the ranges described

377   in Section 2.

378   ii. The piezometric readings are compared to examine possible pumping influences which need to be taken into account in the

379   model by means of a simple abstraction pattern. Based on what is known about nearby abstractions an appropriate pumping

380   depth interval is determined. The magnitude of the extraction rate is manually adjusted as a fitting parameter.

381   iii. Where a piezometer is uninfluenced by pumping we test its behaviour as a geological weighing lysimeter. The heads in the

382   chosen piezometer are assumed to define the mechanical load at the surface, and this assumption is tested for self-consistency

383   by comparison of the simulations to the data from all three piezometers.

384   iv. The nature of the upper head boundary is then examined by reference to the implications for a variety of hydraulic loading

385   conditions. For a 'WT' boundary, changing S_y manually as a fitting parameter adjusts the magnitude of the applied heads

386   concomitant with the mechanical load.

387   **4.1 Groundwater levels at Khulna, south-west Bangladesh**

388   At Khulna town (Burgess et al., 2014) piezometers KhPZ60, KhPZ164 and KhP271 (the numbers indicate depth to the

389   piezometer screen in metres) are located 700 m from the ~300 m wide tidal Rupsa River, in a grassy compound which also

390   contains municipal water-supply pumping boreholes (Supporting Information). The lithological sequence (Fig. 6) comprises a

391   surface clay layer overlying sand in which KhPZ60 is screened, and a deeper layer of clay at 100 m separating the shallow

392   sand from a deeper sand formation in which KhPZ164 and KhPZ271 are screened. Year-round pumping from 250-300 m depth

393   maintains a consistent downward head difference of ~3 m between the uppermost and the lower two piezometers. It is the

394   transient head variations rather than the absolute steady-state head differences that are of interest here. Bodies of standing

395   water in the vicinity, water in the unsaturated zone, and shallow groundwater combine with the sinuous Rupsa River as sources

396   of TWS load; groundwater pumping is an additional source of hydraulic variation.

397

398   The three Khulna hydrographs are characterised by periodic variations containing tidal frequency components throughout the

399   rising and falling limb of the annual cycle, and a series of episodic increments superimposed on the rising limb during the

400   monsoon season; the annual amplitude of groundwater head variation is ~2.5 m. Amplitude of the tidal frequency components

401   increases between 60 m and 164 to 271 m depth, with no phase lag and with a consistent synchroneity between the piezometer

402   heads and the Rupsa River water level fluctuations including the semi-diurnal and spring-neap cycles (Fig. 6 and Supporting

403   Information). Episodic deflections on the hydrograph rising limbs, coincident with rainfall events, are likewise simultaneous

404   at all measurement depths (Burgess et al., 2014). Therefore by reference to the partial coupling analysis (Figures 4 and 5) it is

405   evident that heads in the Khulna piezometers respond primarily to mechanical loading by a combination of monsoon water

406   and tidal loading.

407

At a daily level the time series of groundwater heads in KhPZ164 and KhPZ271 include an additional frequency component which simple analysis of head differences confirms as the hydraulic influence of the daily municipal pumping schedule from which KhPZ60 is protected by an intermediate clay layer. Therefore KhPZ60 alone is taken as recording a solely mechanical loading response and the KhPZ60 head record is applied as the upper boundary condition to represent the varying TWS load at the surface in a 1D hydro-mechanical model of the Khulna site (Fig. 6), assuming ξ =1. The upper boundary resolves all sources of load acting at the site including from the Rupsa River, which is a linear rather than an areally-extensive load. The ratio of daily (tidal) variability in head at KhPZ60 and in the Rupsa River level is ~0.06. At an equivalent loading efficiency, the 1.23 m annual variation in river stage would explain ~0.07 m head variation in KhPZ60, only 3% of the total. While the response of KhPZ60 to the annual changes of the Rupsa River may be greater than to the tidal changes, depending on the details of aquifer structure and hydraulic connection to the river, 97% of the annual variation in head at the piezometer is taken here as attributable to changes in TWS other than load transmitted from the river, representing areally-extensive loads as required by the 1D partially-coupled analysis. This is likely an over-estimate; measurements of true water table fluctuation and surface flooding depths in the vicinity are necessary to constrain the hydro-mechanical model more closely. Given the relatively well-drained urban context at Khulna and the absence of areally-extensive open water that otherwise characterises the rural areas of the GBM floodplains, a 'WT' condition is most likely the dominant loading style, but other sources of loading may also contribute. The layered structure of the Khulna model (Fig. 6) has clay at 0-50 m and 100-150 m with sand in between. The daily municipal pumping cycle is implemented as a source term of 2.4 m a^{-1} for 12 hours of each day applied over the interval 200 to 350 m, the rate having been manually adjusted by reference to the daily head fluctuations in KhPZ164 and KhPZ271.
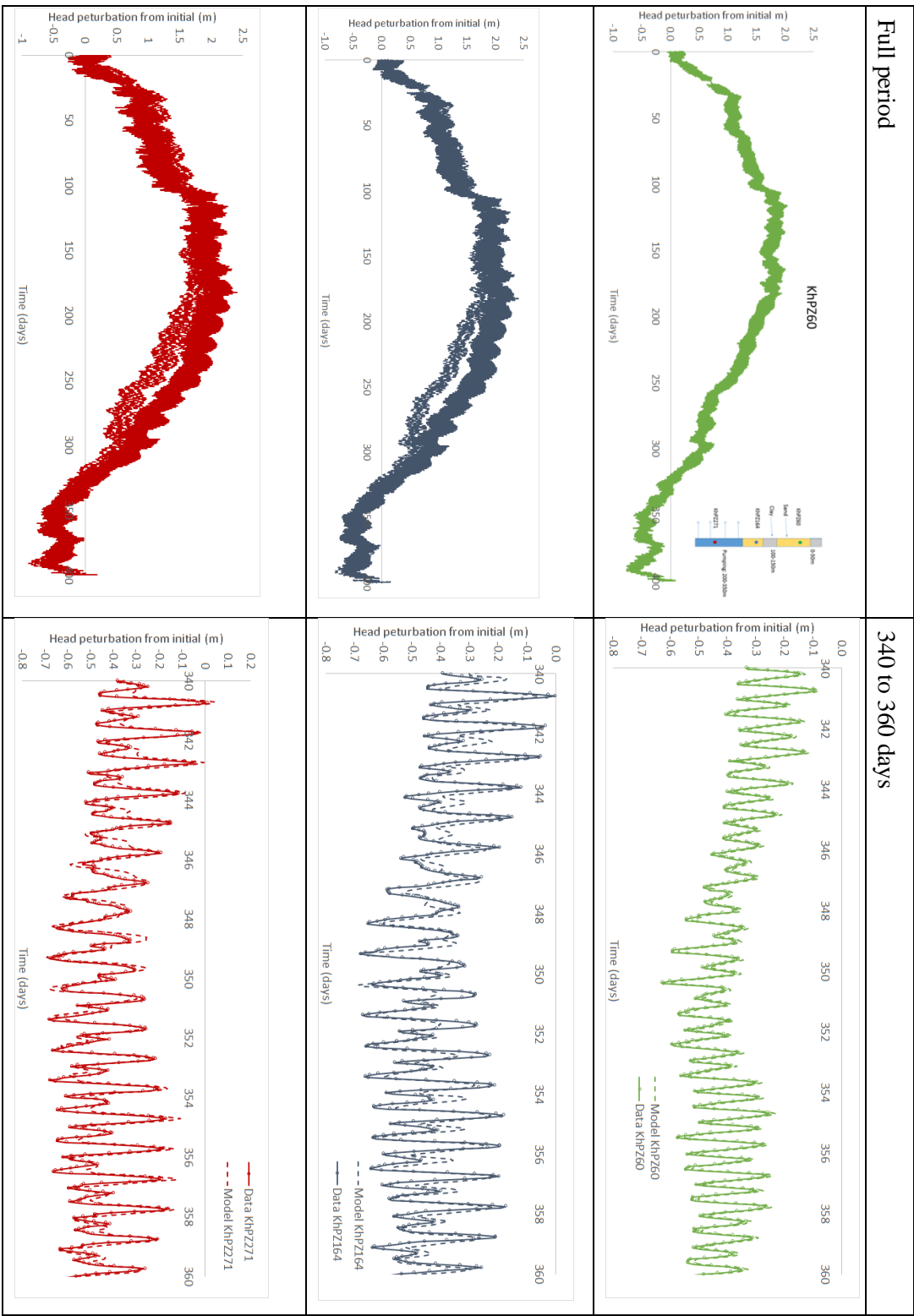
Figure 6. Khulna: comparison of observed heads (solid lines) and simulated heads (dashed lines), starting 27 April 2013, for WT upper boundary condition (S_y=0.4). X-axis is time in days. The surface loading is set equal to the observed head in KhPZ60, and the surface head is set to the observed head in KhPZ60 divided by S_y. The pumping rate is 2.4 m a^{-1} for 12 hours of each day, switching on at 05:45 am. Top (green) is KhPZ60, middle (blue) is KhPZ164, bottom (red) is KhPZ271.

438

439 Figure 6 compares the measured groundwater heads with the heads simulated by the model under the assumption of a 'WT'

440 boundary with S_y assigned a value of 0.4, with $\kappa_{sand} = 1 \times 10^{-5}$ m s^{-1}, $\kappa_{clay} = 1 \times 10^{-9}$ m s^{-1}, $S_S = 10^{-4}$ m^{-1} (corresponding to

441 E=82.07 MPa), $\nu = 0.25$ and $n = 0.1$. The results are insensitive to S_y being varied in the range from 0.1 to 1 (the latter being

442 equivalent to an 'IN' boundary), and are near-identical in the case of a 'LD' boundary (Supporting Information). This is

443 because the upper clay effectively isolates the piezometers from the surface hydraulically.

444 **4.2 Groundwater levels at Laksmipur, south-east Bangladesh**

445 At Laksmipur (Burgess et al., 2017) the piezometers LkPZ91, LkPZ152 and LkPZ244 are situated in a rural region of rice-

446 paddy and tree plantations on the Lower Meghna floodplain (Supporting Information), 10 km distant from the River Meghna

447 and 8 km from municipal boreholes which pump from 270–300 m depth. Seasonal pumping from depths up to 100 m for rice

448 irrigation is common in the vicinity. The lithological sequence indicates fine sand with occasional silty clay layers. The

449 hydrographs are characterised by a sequence of episodic increments in groundwater head associated with periods of heavy

450 rainfall producing a rising limb of amplitude ~1 m through the monsoon season; during the dry-season recession, minor

451 periodic fluctuations of order 0.01 m containing atmospheric frequency components become more clearly evident (Burgess et

452 al., 2017). The episodic increments are almost synchronous and of consistent magnitude at all piezometer depths, indicative

453 by reference to Figures 4 and 5 of groundwater heads responding dominantly to mechanical loading and unloading due to

454 changes in TWS above the aquifer surface.

455

456 Here, cyclical head differences between LkPZ244 and the shallower two piezometers indicate hydraulic influences of dry-

457 season pumping on the LkPZ91 and LkPZ152 hydrographs, whereas downward propagation of the hydraulic signals to

458 LkPZ244 is prevented by the clay layer at 170 m depth. Therefore LkPZ244 is taken as recording a solely mechanical loading

459 response and the LkPZ244 head record is applied as the upper boundary condition to represent the varying TWS load at the

460 surface in a 1D hydro-mechanical model of the Laksmipur site (Fig. 7), with a small offset applied to the initial heads above

461 170 m depth, consistent with the observed head perturbations being shown as starting from a common zero value. The

462 stratigraphy as modelled draws from the detail of the drillers log at Laksmipur (Burgess et al., 2017) and the general form of

463 the stratigraphy as seen across the GBM floodplains (Fig. 2). All styles of upper boundary were applied ('IN', 'LD', and 'WT'

464 with a range of S_y values, see Supporting Information) in an attempt to distinguish the dominant source of TWS load around

465 the site from the boundary style leading to the best fit with piezometer measurements. In all other respects the models

466 incorporate the dimensions and assumptions as described in Sect. 3, with sand ($\kappa_{sand} = 1 \times 10^{-5}$ m s^{-1}) and two clay layers

467 (BWDB, 2013) at 25-30 m and 170-200 m ($\kappa_{clay} = 1 \times 10^{-8}$ m s^{-1}), and E=82.07 MPa. A simple dry-season pumping regime

468 over a 105 day period starting 17 November 2013 is implemented as a source term of 0.04 m a^{-1} applied over the interval 30

469 to 70 m in the model, manually adjusted by reference to the LkPZ91 and LkPZ152 hydrographs.

470

471
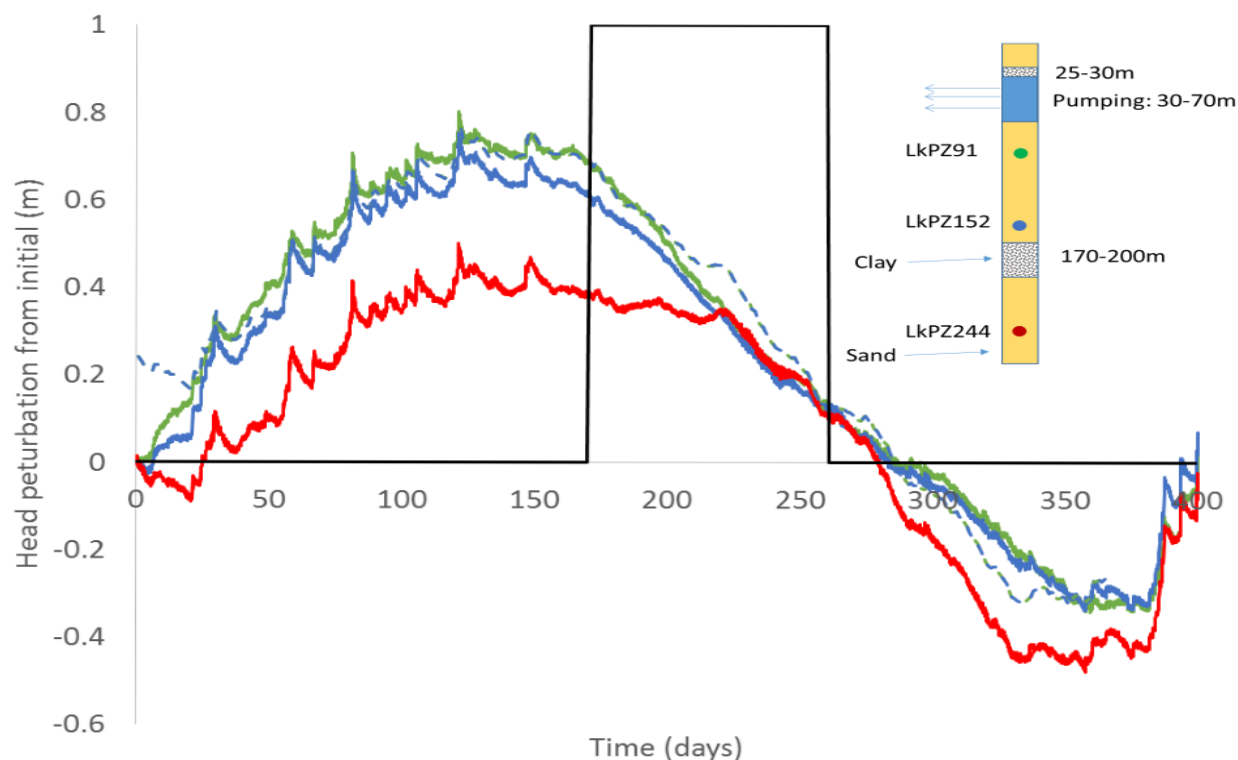
Figure 7. Laksmipur: comparison of observed heads (solid lines) and simulated heads (dashed lines) starting 31 May 2013, for 'WT' upper boundary condition (S_y=0.8), for LkPZ91 (green), LkPZ152 (blue) and LkPZ244 (red). X axis is time in days. The surface loading is set equal to the observed head in LkPZ244, and the surface head is set to the observed head in LkPZ244 divided by S_y. The pumping rate is 0.04 m a^{-1} for the period shown (1 for 'on', 0 for 'off').

476

For LkPZ244 the simulated heads are an excellent match with measurements over the entire period. The simulated heads for the shallower two piezometers LkPZ91 and LkPZ152 most closely match the measurements under a 'WT' boundary with S_y assigned a value of 0.8 (Fig. 7 and Supporting Information). The model results therefore confirm that LkPZ244 is isolated from the hydraulic effects of water table variation and of seasonal pumping, and the LkPZ244 groundwater head variation over the observation period is determined solely by mechanical loads at the surface. Therefore LkPZ244 is validated as acting effectively as a geological weighing lysimeter (Burgess et al., 2017).

For the shallower piezometers, the best fit value for S_y is higher than is reasonable for fine sand and more likely indicates the combined effects of a variable water table and fluctuating levels of standing water, in drainage channels and on paddy fields around the piezometer site, consistent with the field situation. As a consequence of seasonal pumping at 0.04 m a^{-1}, the model

487 shows groundwater is both drawn from storage and induced as recharge from the upper surface, but the amplitude of saturated

488 storage fluctuation is only 6 mm, therefore changes to the water budget are dominated by recharge to the water-table. The

489 surface displacement is predicted at 6 mm amplitude, in phase with the changes in storage.

5 Discussion

490

5.1 Aquifer responses to discrete modes of terrestrial water variation

491

492 Models based on the 1D partially-coupled hydro-mechanical analysis confirm that substantial poroelastic influences should be

493 expected in the Bengal Aquifer System, and that groundwater heads respond characteristically to changes in specific terrestrial

494 water stores (Figures 4 and 5). Only laterally-extensive flooding above an aquifer fully saturated to the ground surface (the

495 'IN' loading style) will drive instantaneous and synchronous head variations at all depths determined by the loading efficiency,

496 inducing negligible flow of groundwater. In any situation involving a variable water table (the 'WT' loading style) and for any

497 variable loads hydraulically disconnected from the aquifer (the 'LD' style), hydraulic gradients are imposed due to the unequal

498 magnitude of stress and head at the surface. These gradients take time to dissipate, depending on the frequency of the signal

499 fluctuation and the aquifer hydraulic diffusivity, and so lead to differences in amplitude and phase of the head response with

500 depth. In these situations, the relative importance of the hydraulic and mechanical influence is controlled by the aquifer

501 hydraulic diffusivity, the loading efficiency and the depth of interest. In the case of a fluctuating water table, the difference

502 between the head and stress signals is a function of the specific yield, S_y, in the zone of fluctuation.

503

504 The characteristic responses of the aquifer might therefore provide a key to identifying the terrestrial water store dominating

505 ΔTWS, by monitoring vertical profiles of groundwater head. Multiple terrestrial water stores will normally contribute,

506 however, as at Laksmipur and Khulna, so a unique identification may not be possible. This limitation is inherent to the 1D

507 analysis, which resolves all the contributions to load into one upper boundary condition respectively for head and stress. The

508 analysis indicates how different loads and dynamic responses superpose to produce the observed groundwater hydrographs. In

509 principle, key aspects of the water balance may be better estimated by de-convolving known components of the ΔTWS signal.

510 Anochikwa et al. (Anochikwa et al., 2012) assembled field measurements of rainfall and evapotranspiration at a site in

511 Saskatchewan, Canada, using them to define the upper boundary conditions in a one-dimensional model to examine their

512 hydraulic and mechanical loading separately, before summing the outcomes to simulate the overall hydro-mechanical influence

513 on groundwater pressure. Having determined loading efficiency by reference to barometric effects, they then calibrated their

514 1D model against observed groundwater pressures by varying hydraulic conductivity. At Khulna and Laksmipur,

515 measurements of the separate components of the terrestrial water cycle were not available, hence an indirect demonstration of

516 hydro-mechanical effects was desirable. The simulated and observed heads are in good agreement, consistent with the local

517 conditions, so confirming the 1D partially-coupled analysis as a suitable basis for representing the poroelastic behaviour of the

518 BAS.

5.2 Significance for groundwater monitoring and geological weighing lysimetry

In terms of the extent to which piezometer water levels indicate recharge and drainage, it is only where there is a rapid hydraulic connection between the piezometer and the water table that the piezometer will be sensitive to head change at the water table and therefore to changes in unconfined storage. If a piezometer is hydraulically isolated from surface water and/or the water table and is beyond other transient hydraulic influences, it can respond to changes in the weight of the TWS load, acting as a geological weighing lysimeter (van der Kamp and Maathuis, 1991;Smith et al., 2017). In this case, where the changing load is due to a moving water table, knowledge of the loading efficiency allows the load measurement to be converted into an estimate of recharge and discharge.

In all other situations, a wide range of coupled hydro-mechanical responses can be expected, as we have shown for the BAS (Figures 4 and 5). Seasonally-variable groundwater heads (Fig. 4) are therefore open to misinterpretation as seasonally-variable groundwater storage, leading to error in determination of recharge if the poroelastic nature of the response is neglected. Consider heads at 30 m, a common depth for Bangladesh Water Development Board (BWDB) monitoring boreholes (Shamsudduha et al., 2011). For the case of a variable load hydraulically disconnected from the aquifer (Fig. 4d) the annual water level rise is equal to half the amplitude of the load yet augmentation of elastic storage, by definition in this case, is nil. For the case of variable TWS inundation (Fig. 4a) the annual groundwater level rise is equivalent to the annual depth of inundation yet augmentation of elastic and unconfined storage is insignificant. Conversely, relative to a variable water table (Fig. 4b,c) groundwater fluctuation at 30 m depth is attenuated. Failure to account for this would lead to an underestimate of recharge to unconfined storage by about 30%. The error increases as hydraulic diffusivity decreases, therefore errors could be expected to be greater in the coastal regions of the Bengal Basin where the thickness of silty-clays is greater (Mukherjee et al., 2007). Considerable caution is therefore necessary in the use of even relatively shallow piezometers as indicators of recharge to the water table. A true indication of recharge requires either a shallow tubewell screened over the depth interval of actual water table fluctuation, or a deep piezometer responding as a geological weighing lysimeter to the varying mass provided by a fluctuating water table. In the latter case it is recharge to the shallow water table that is measured, not recharge at the depth of the piezometer.

The 1D hydro-mechanical framework can be applied as a test for the special cases where groundwater head responds solely to mechanical load, and hence to validate the use of geological weighing lysimetry. The laterally-extensive loading criterion inherent to the 1D analysis must apply, and the piezometer screen must be isolated or distant from hydraulic transients originating at the surface or from pumping. We have shown for the BAS that these requirements most likely occur at depths beyond about 250 m, as in the case of 'WT' and 'LD' loading styles in the absence of pumping (Fig. 5). The inundation ('IN') style of TWS variation leads to instantaneous transmission of head without loss of amplitude at all depths; in this case piezometers at all depths provide a mechanical record of ΔTWS rather than a hydraulic record of storage variation and to infer

552 recharge would lead to 100% error. Our analysis demonstrates a solely mechanical loading response at 244 m depth at
553 Laksmipur, below the level of seasonal irrigation pumping, and at 60 m depth at Khulna, above the level of deep pumping for
554 municipal water supply.

5.3 Significance for ground surface displacements and groundwater storage changes

556 The models also demonstrate the amplitude and phase of ground surface displacement as a hydro-mechanical consequence of
557 varying terrestrial water stores, and the significance of pumping (Fig. 4e and 4f). Under simplifications associated with the 1D
558 model, vertical surface displacements relative to a fixed model base at 1 km depth are approximately equal to the change in
559 elastic storage, the small difference being due to compressibility of water. These changes are minor in the BAS under all TWS
560 loading styles, in the order of mm, compared to the displacements in the case of seasonal groundwater pumping which are in
561 the order of cm. Seasonal surface displacements in the order of cm have also been attributed to strain acting over a depth scale
562 of hundreds of kilometres due to the load applied by monsoonal inundation over the entire Bengal Basin (Steckler et al., 2010).
563 Strains due to seasonal groundwater pumping at shallow depths may therefore be in the same order of magnitude but out of
564 phase with crustal stain, making ground surface deflections a poor proxy for changing elastic storage in the aquifer. As a
565 corollary, interpretation of seasonal ground surface fluctuations across the GBM floodplains solely in terms of deep crustal
566 deformation (Steckler et al., 2010) potentially requires reassessment in the light of BAS aquifer poroelasticity.

5.4 Limitations and further consequences

568 In our analysis we have based values for the 1D loading efficiency, ξ (0.932-0.993) and Young's Modulus, E (82-851 MPa)
569 in the BAS on field measurements of S_s, for the sake of internal hydro-mechanical consistency, but we have noted a discrepancy
570 with lower values for the 1D loading efficiency ξ (0.69-0.87) derived from determinations of barometric efficiency (Burgess
571 et al., 2017). These differences require attention, but the overall conclusions on the significance of poroelastic behaviour in
572 the BAS and the pattern of poroelastic responses characteristic of specific upper surface TWS boundary conditions are
573 unaffected. Although we omitted barometric effects in the generic simulations for the sake of simplicity, it is straightforward
574 to superpose a further loading signal on top of the existing one if required, as for example when deconvolving deep piezometric
575 signals to make water resources assessments (Anochikwa et al., 2012).
576 Data on changes of the water table would have greatly helped the analysis of loading effects at Khulna and Laksmipur. It is
577 strongly recommended that in future hydro-mechanical analyses of the groundwater dynamics of large layered aquifers such
578 as the BAS, both water table data and deeper head data should be obtained. For the water table, this requires a shallow
579 piezometer to be screened across the full range of fluctuation of the true water table.
580
581 Under certain circumstances the extensive load assumption inherent in the 1D analysis may break down. Rivers, as linear
582 sources of head and load, can be accommodated within the 1D framework where their contribution to the TWS load is minor
583 as demonstrated at Khulna. In general however, rivers should be expected to impose laterally variable heads and require a

584 more generalised 2D or 3D fully-coupled poro-mechanical treatment (Boutt, 2010;Pacheco and Fallico, 2015). An equivalent

585 constraint applies to strains, an additional reason for surface displacement not to offer a secure proxy for groundwater storage

586 in the BAS. The dense distribution of rivers, distributaries and drainage channels in the Bengal Basin makes the BAS widely

587 vulnerable to loading effects that may not adequately be reduced to a 1D description; 13% and 47% of 1035 piezometers in

588 the BWDB groundwater monitoring network lie within 1 and 5 km respectively of a river.

589 **6 Conclusions**

590 We argue that a 1D *partially-coupled* approach to hydro-mechanical processes, whereby the loading term is included in the

591 flow equation without the need to simultaneously compute the elastic equation, is a suitable basis for representing the

592 poroelastic behaviour of the Bengal Aquifer System when surface conditions can be treated as areally extensive. Applying a

593 1D *partially-coupled* hydro-mechanical analysis we have shown how the BAS responds characteristically to specific sources

594 of terrestrial water storage variation. Rivers can be incorporated as a component of the 1D load where their contribution is

595 small, but in general will require a 2D or fully 3D treatment.

596

597 Groundwater levels, groundwater recharge, vertical groundwater flow and ground surface elevations are all influenced by the

598 poroelastic behaviour of the BAS. Our results expose the error of the conventional assumption of de-coupled hydraulic

599 behaviour which underlies previous assessments of recharge to the BAS. Also they demonstrate the complexities in applying

600 ground surface displacements as a proxy measure for variations in groundwater storage. We propose that the 1D *partially-*

601 *coupled* analysis can be applied to validate when geological weighing lysimetry is applicable in the BAS. In some situations,

602 geological weighing lysimetry offers an alternative approach to recharge assessment.

603

604 **Appendix: Poromechanical equations**

605 The constitutive isotropic relation between elastic stress and strain, coupled to the pore-pressure by Terzaghi's effective stress

606 law is given by (Neuzil, 2003):

$$\sigma_{ij} = 2G\varepsilon_{ij}\delta_{ij} + 2G\frac{\nu}{1-2\nu}\varepsilon_{kk}\delta_{ij} + \alpha_B p\delta_{ij} \qquad \text{(A1)}$$

607 where δ_{ij} is the Kronecker delta (which is zero when $i \neq j$ and one when $i = j$) and following the Einstein Summation

608 convention; stresses (σ_{ij}) and strains (ε_{ij}) are positive in compression; p is the porewater pressure (Pa), ν is Poisson's ratio (-

609), G is the shear modulus (MPa), and $\alpha_B = 1 - K/K_s$, where, K (MPa) is the bulk modulus of the porous medium and K_s

610 (MPa) is the bulk modulus of the solid grains.

611

612 Just as the elastic equations have a pore pressure term, the isothermal, Darcian groundwater flow equation contains a coupled

613 stress term (Neuzil, 2003):

$$\nabla \cdot \kappa (\nabla p + \rho g \nabla z) = S_{s3} \frac{\partial p}{\partial t} - S_{s3} \beta \frac{\partial \sigma_t}{\partial t} - gJ \tag{A2}$$

614   where κ is the hydraulic conductivity (m s^{-1}), p is the pore pressure (Pa), z is the elevation (m), J is a source term used here

615   to simulate groundwater abstraction by pumping and $\sigma_t = (\sigma_{xx} + \sigma_{yy} + \sigma_{zz})/3$ (Pa).

616

617   The 3D specific storage is defined as:

$$S_{s3} = \rho g \left[\left(\frac{1}{K} - \frac{1}{K_s} \right) + \left(\frac{n}{K_f} - \frac{n}{K_s} \right) \right] \tag{A3}$$

where n is the porosity, and K_f is the modulus of the water (MPa).

The (3D) loading efficiency, or Skempton's coefficient, β, is defined as:

$$\beta = \frac{\left(\frac{1}{K} - \frac{1}{K_s} \right)}{\left(\frac{1}{K} - \frac{1}{K_s} \right) + \left(\frac{n}{K_f} - \frac{n}{K_s} \right)} \tag{A4}$$

618   Where there is areally extensive loading, the 1D loading efficiency is given by

$$\xi = \beta(1 + \nu)/[3(1 - \nu) - 2\alpha_B \beta(1 - 2\nu)] \tag{A5}$$

619

620   The 1D specific storage is given by:

$$S_s = S_{s3}(1 - \lambda \beta) \tag{A6}$$

621   where $\lambda = 2\alpha_B(1 - 2\nu)/3(1 - \nu)$.

622   **Author contributions**

623   WGB conceived the study; NDW led the modelling; all authors contributed to the scenario descriptions and consideration of

624   the modelling results; NDW and WGB drafted the manuscript; all authors reviewed the manuscript.

625

626   **Acknowledgments**

627   We acknowledge funding from the UK EPSRC Global Challenges Research Fund (UCL/BEAMS EPSRC GCRF award

628   172313) to WGB for research on *Poroelasticity in the Bengal Aquifer System and groundwater resources monitoring in*

629   *Bangladesh.* NDW thanks the University of Southampton for leave of absence during the course of the project. Field

630   measurements at Khulna and Laksmipur were made with the kind assistance of the Bangladesh Water Development Board

631   (BWDB) and financial support from the UK Department for International Development (DfID) under the project *Groundwater*

632   *Resources in the Indo-Gangetic Basin* (Grant 202125-108) managed by Professor Alan MacDonald of the British Geological

633   Survey. We are grateful to Professors Mike Steckler, Columbia University, and Humayun Akhter, Dhaka University, for useful

634   discussions on ground surface vertical motions in the Bengal Basin, and to John Barker and William Powrie for helpful

635   discussion of the fundamental processes at the start of the research. Dr. Mohammed Shamsudduha, University College London,

636   and Ms. Sarmin Sultana, Dhaka University are thanked for discussions on the hydrological context of the groundwater level

637   monitoring piezometers. The data used are listed in the references and illustrated in the Supporting Information. We thank one

638   anonymous reviewer whose comments and advice helped improve the manuscript.

639   **Nomenclature**

640   α Proportion of mechanical load as head

641   α_B Biot-Willis coefficient, $1 - K/K_s$

642   β, C 3D loading efficiency, Skempton's coefficient, or 'tidal efficiency'

643   δ_{ij} Kronecker delta

644   ε_{ij} Strain

645   θ $z\sqrt{\dfrac{\omega}{2D}} = z\sqrt{\dfrac{\pi}{DT}}$

646   λ $2\alpha_B(1 - 2\nu)/3(1 - \nu)$

647   ν Poisson's ratio

648   ξ 1D loading efficiency

649   κ Hydraulic conductivity

650   ρ Water density

651   σ_{ij} Stress tensor

652   σ_t Total stress

653   ψ Lag (radians)

654   ω Angular frequency

655

656   a River half-width

657   B Barometric efficiency

658   E Young's Modulus

659   D Hydraulic diffusivity

660   g Acceleration due to gravity

661   G Shear Modulus

662   h Head

663	$H(t)$	Top boundary head
664	H_0	Amplitude of top boundary head
665	J	Fluid source term
666	K	Bulk Modulus of porous medium
667	K_f	Bulk modulus of the water
668	K_s	Bulk modulus of the solid grains
669	$L(t)$	Top boundary load
670	L_0	Amplitude of top boundary load
671	n	Porosity
672	p	Pore pressure
673	S_y	Specific Yield
674	S_s	Specific storage
675	S_{s3}	3D Specific storage
676	t	Time
677	u	Vertical displacement
678	x	Perpendicular distance from a river
679	z	Vertical coordinate
680		

References

682
683 COMSOL Multiphysics® v. 5.2. www.comsol.com. . COMSOL AB, Stockholm, Sweden.
684 Acworth, R. I., Rau, G. C., McCallum, A. M., Andersen, M. S., and Cuthbert, M. O.: Understanding connected surface-
685 water/groundwater systems using Fourier analysis of daily and sub-daily head fluctuations, Hydrogeology Journal, 23, 143-
686 159, 10.1007/s10040-014-1182-5, 2015.
687 Anochikwa, C. I., van der Kamp, G., and Barbour, S. L.: Interpreting pore-water pressure changes induced by water table
688 fluctuations and mechanical loading due to soil moisture changes, Canadian Geotechnical Journal, 49, 357-366, 2012.
689 Bakker, M.: The effect of loading efficiency on the groundwater response to water level changes in shallow lakes and
690 streams, Water Resources Research, 52, 1075-1715, doi:10.1002/2015WR017977, 2016.
691 Bardsley, W. E., and Campbell, D. J.: A new method for measuring near-surface moisture budgets in hydrological systems,
692 Journal of Hydrology, 154, 245-254, 1994.
693 Bardsley, W. E., and Campbell, D. J.: Natural geological weighing lysimeters: calibration tools for satellite and ground
694 surface gravity monitoring of subsurface water-mass change, Natural Resources Research, 9, 147-156, 2000.
695 Bardsley, W. E., and Campbell, D. J.: An expression for land surface water storage monitoring using a two-formation
696 geological weighing lysimeter, Journal of Hydrology, 335, 240-246, 2007.
697 Barr, A. G., van der Kamp, G., Schmidt, R., and Black, T. A.: Monitoring the moisture balance of a boreal aspen forest using
698 a deep groundwater piezometer, Agricultural and Forest Meteorology, 102, 13-24, 2000.
699 Benner, S. G., Polizzotto, M. L., Kocar, B. D., Ganguly, S., Phan, K., Ouch, K., Sampson, M., and Fendorf, S.: Groundwater
700 flow in an arsenic-contaminated aquifer, Mekong Delta, Cambodia, Applied Geochemistry, 23, 3072-3087, 2008.

Bense, V. F., and Person, M. A.: Transient hydrodynamics within intercratonic sedimentary basins during glacial cycles, Journal of Geophysical Research:Earth Surface (2003-2012), 113, 2008.

Black, J. H., and Barker, J. A.: The puzzle of high heads beneath the West Cumbrian coast, UK: a possible solution, Hydrogeology Journal, 24, 439-457, 10.1007/s10040-015-1340-4 2016.

Boutt, D. F.: Poroelastic loading of an aquifer due to upstream dam releases, Ground Water, 48, 580-592, 2010.

Burbey, T. J., Warner, S. M., Blewitt, G., Bell, J. W., and Hill, E.: Three-dimensional deformation and strain induced by municipal pumping, part 1: Analysis of field data, Journal of Hydrology, 319, 123-142, 2006.

Burgess, W. G., Hoque, M. A., Michael, H. A., Voss, C. I., Breit, G. N., and Ahmed, K. M.: Vulnerability of deep groundwater in the Bengal Aquifer System to contamination by arsenic, Nature Geoscience, 3, 83-87, 10.1038/ngeo750, 2010.

Burgess, W. G., Shamsudduha, M., Taylor, R. G., Zahid, A., Ahmed, K. M., Mukherjee, A., and Lapworth, D. J.: Seasonal, episodic and periodic changes in terrestrial water storage recorded by deep piezometric monitoring in the Ganges/Brahmaputra/Meghna delta, AGU Fall Meeting 2014, San Francisco, 2014.

Burgess, W. G., Shamsudduha, M., Taylor, R. G., Zahid, A., Ahmed, K. M., Mukherjee, A., Lapworth, D. J., and Bense, V. F.: Terrestrial water load and groundwater fluctuation in the Bengal Basin, Scientific Reports, 7(1), 3872, 10.1038/s41598-017-04159-w, 2017.

BWDB: Establishment of monitoring network and mathematical model study to assess salinity intrusion in groundwater in the coastal area of Bangladesh due to climate change. Final report. Bangladesh Water Development Board, Dhaka, 773, 2013.

Chaussard, E., Burgmann, R., Shirzaei, M., Fielding, E. J., and Baker, B.: Predictability of hydraulic head changes and characterization of aquifer-system and fault properties from InSAR-derived ground deformation, Journal of Geophysical Research: Solid Earth, 119, 6572–6590, 10.1002/2014JB011266, 2014.

de Silva, S., Wightman, N. R., and Kamruzzaman, M.: Geotechnical ground investigation for the Padma Main Bridge, IABSE-JSCE Joint Conference on Advances in Bridge Engineering-II, Dhaka, Bangladesh, 2010,

Domenico, P. A., and Schwartz, F. W.: Physical and Chemical Hydrogeology, 2nd ed., John Wiley & Sons, New York, 1998.

Erban, L. E., Gorelick, S. M., and Zebker, H. A.: Groundwater extraction, land subsidence, and sea-level rise in the Mekong Delta, Vietnam, Environmental Research Letters, 9, 10.1088/1748-9326/9/8/084010, 2014.

Fendorf, S., Michael, H. A., and van Geen, A.: Spatial and temporal variations of groundwater arsenic in south and southeast Asia, Science, 328, 1123-1127, 2010.

Gibson, R. E.: The analytical method in soil mechanics, Geotechnique, 24, 115-140, 1974.

Green, D. H., and Wang, H. F.: Specific storage and poroelastic coefficient, Water Resources Research, 26, 1631-1637, 1990.

Hasanuzzaman, S. M.: Impact of groundwater utilisation on agriculture, in: Groundwater resources and development in Bangladesh: background to the arsenic crisis, agricultural development and the environment, edited by: Rahman, A. A., and Ravenscroft, P., Bangladesh Centre for Advanced Studies, University Press Ltd., Dhaka, 161-185, 2003.

Hoque, M. A., Burgess, W. G., and Ahmed, K. M.: Integration of aquifer geology, groundwater flow and arsenic distribution in deltaic aquifers – A unifying concept, Hydrological Processes, 31, 2095-2109, https://doi.org/10.1002/hyp.11181, 2017.

Hussain, M. M., and Abdullah, S. K. M.: Geological setting of the areas of arsenic safe aquifers. Report of the ground water task force, Ministry of Local Government, Rural Development & Cooperatives, Local Government Divison, BangladeshInterim Report No. 1, 2001.

Jacob, C. E.: On the flow of water in an elastic artesian aquifer, Transactions of the American Geophysical Union, 574-586, 1940.

Lambert, A., Huang, J., van der Kamp, G., Henton, J., Mazzotti, S., James, T. S., Courtier, N., and Barr, A. G.: Measuring water accumulation rates using GRACE data in areas experiencing glacialisostatic adjustment: The Nelson River basin, Geophysical Research Letters, 40, 6118-6122, 10.1002/2013GL057973, 2013.

Larsen, F., Pham, N. Q., Dang, N. D., Postma, D., Jessen, S., Pham, V. H., Nguyen, T. B., Trieu, H. D., Tran, L. T., Nguyen, H., Chambon, J., Nguyen, H. V., Ha, D. H., Hue, N. T., Duc, M. T., and Refsgaard, J. C.: Controlling geological and hydrogeological processes in an arsenic contaminated aquifer on the Red River flood plain, Vietnam, Applied Geochemistry, 23, 3099-3115, 2008.

751 Manga, M. I., Beresnev, I., Brodsky, E. E., Elkhoury, J. E., Elsworth, D., Ingebritsen, S. E., Mays, D. C., and Wang, C.-Y.:
752 Changes in permeability caused by transient stresses: field observations, experiments, and mechanisms, Reviews of
753 Geophysics, 50, 10.1029/2011RG000382, 2012.
754 Marin, S., van der Kamp, G., Pietroniro, A., Davison, B., and Toth, B.: Use of geological weighing lysimeters to calibrate a
755 distributed hydrological model for the simulation of land-atmosphere moisture exchange, Journal of Hydrology, 383, 179-
756 185, 2010.
757 Michael, H. A., and Voss, C. I.: Evaluation of the sustainability of deep groundwater as an arsenic-safe resource in the
758 Bengal Basin, PNAS, 105, 8531-8536, 2008.
759 Michael, H. A., and Voss, C. I.: Estimation of regional-scale groundwater flow properties in the Bengal Basin of India and
760 Bangladesh, Hydrogeology Journal, 17, 1329-1346, 10.1007/s10040-009-0443-1, 2009a.
761 Michael, H. A., and Voss, C. I.: Controls on groundwater flow in the Bengal Basin of India and Bangladesh: regional
762 modeling analysis, Hydrogeology Journal, 17, 1561-1577, 10.1007/s10040-008-0429-4, 2009b.
763 Mukherjee, A., Fryar, A. E., and Rowe, H. D.: Regional hydrostratigraphy and groundwater flow modeling of the arsenic
764 affected western Bengal basin, West Bengal, India, Hydrogeology Journal, 15, 1397-1418, 10.1007/s10040-007-0208-7,
765 2007.
766 Narasimhan, T. N.: On storage coefficient and vertical strain, Ground Water, 44, 488-491, 2006.
767 Neuzil, C. E.: Hydromechanical coupling in geological processes, Hydrogeology Journal, 11, 41-83, 2003.
768 Pacheco, F. A. L., and Fallico, C.: Hydraulic head response of a confined aquifer influenced by river stage fluctuations and
769 mechanical loading, Journal of Hydrology, 531, 716-727, http://dx.doi.org/10.1016/j.jhydrol.2015.10.055, 2015.
770 Powrie, W.: Soil Mechanics: Concepts and Applications, 3rd ed., CRC Press, Taylor and Francis Group, Boca Raton,
771 Florida, 2014.
772 Rahman, M. A. T., Majumder, R. K., Rahman, S. H., and Halim, M. A.: Sources of deep groundwater salinity in the
773 southwestern zone of Bangladesh, Environmental Earth Sciences, 63, 363-373, 2011.
774 Ravenscroft, P.: Overview of the hydrogeology of Bangladesh, in: Groundwater resources and development in Bangladesh:
775 background to the arsenic crisis, agricultural potential and the environment, edited by: Rahman, A. A., and Ravenscroft, P.,
776 Bangladesh Centre for Advanced Studies, University Press Ltd., Dhaka, 43-86, 2003.
777 Ravenscroft, P., Burgess, W. G., Ahmed, K. M., Burren, M., and Perrin, J.: Arsenic in groundwater of the Bengal Basin,
778 Bangladesh: Distribution, field relations, and hydrogeological setting, Hydrogeology Journal, 13, 727–751, 10.1007/s10040-
779 003-0314-0, 2005.
780 Ravenscroft, P., Brammer, H., and Richards, K. S.: Arsenic pollution: a global synthesis, First ed., Wiley-Blackwell, UK,
781 616 pp., 2009.
782 Ravenscroft, P., McArthur, J. M., and Hoque, M. A.: Stable groundwater quality in deep aquifers of Southern Bangladesh:
783 The case against sustainable abstraction, Sci Total Environ., 454-455, 627-638, 2013.
784 Reeves, J. A., Knight, R., Zebker, H. A., Kitanidis, P. K., and Schreuder, W. A.: Estimating temporal changes in hydraulic
785 head using InSAR data in the San Luis Valley, Colorado, Water Resources Research, 50, 4459-4473,
786 10.1002/2013WR014938, 2014.
787 Roeloffs, E. A.: Fault stability changes induced beneath a reservoir with cyclic variations in water level, Journal of
788 Geophysical Research, 93, 2107-2124, 1988.
789 Rojstaczer, S., and Agnew, D. C.: The influence of formation material properties on the response of water levels in wells to
790 Earth tides and atmospheric loading, Journal of Geophysical Research, 94, 12,403-412,411, 1989.
791 Shamsudduha, M., Taylor, R. G., Chandler, R. E., and Ahmed, K. M.: Basin-scale variations in shallow groundwater levels
792 in Bangladesh over the last 40 years: assessing the impacts of groundwater-fed irrigation. In: Water scarcity and water
793 security seminar, Geological Society, London, U. K., 2008.
794 Shamsudduha, M., Taylor, R. G., Ahmed, K. M., and Zahid, A.: The impact of intensive groundwater abstraction on
795 recharge to a shallow regional aquifer system: evidence from Bangladesh, Hydrogeology Journal, 19, 901-916,
796 10.1007/s10040-011-0723-4, 2011.
797 Shamsudduha, M., Taylor, R. G., and Longuevergne, L.: Monitoring groundwater storage changes in the highly seasonal
798 humid tropics: validation of GRACE measurements in the Bengal Basin, Water Resour. Res., W02508,
799 10.1029/2011WR010993, 2012.

800 Shamsudduha, M., Zahid, A., and Burgess, W. G.: Security of deep groundwater against arsenic contamination in the Bengal
801 Aquifer System: a numerical modelling study in southest Bangladesh, Sustainable Water Resources Management
802 doi.org/10.1007/s40899-018-0275-z, 2018.
803 Smith, C., van der Kamp, G., Arnold, L., and Schmidt, R.: Measuring precipitation with a geolysimeter, Hydology and Earth
804 System Science, 21, 5263–5272, 2017.
805 Spane, F. A.: Considering barometric pressure in groundwater flow investigations, Water Resources Research, 38,
806 10.1029/2001WR000701, 2002.
807 Steckler, M. S., Nooner, S. L., Akhter, S. H., Chowdhury, S. K., Bettadpur, S., Seeber, L., and Kogan, M. G.: Modeling earth
808 deformation from monsoonal flooding in Bangladesh using hydrographic, GPS and GRACE Data, Journal of Geophysical
809 Research, 115, 10.1029/2009JB007018, 2010.
810 Sultana, S., Ahmed, K. M., Mahtab-Ul-Alam, S. M., Hasan, M., Tuinhof, A., Ghosh, S. K., Rahman, M. S., Ravenscroft, P.,
811 and Zheng, Y.: Low-cost aquifer storage and recovery: implications for improving drinking water access for rural
812 communities in coastal Bangladesh, Journal of Hydrologic Engineersing, 20, B5014007-5014001-5014012,
813 10.1061/(ASCE)HE.1943-5584.0001100., 2015.
814 Sutherland, R., Townend, J., Toy, V., Upton, P., Coussens, J., Allen, M., and etc.: Extreme hydrothermal conditions at an
815 active plate-bounding fault, Nature, 546, 137-140, 10.1038/nature22355, 2017.
816 Tam, V. T., Batelaan, O. L. T. T., and Nhan, P. Q.: Three-dimensional hydrostratigraphical modelling to support evaluation
817 of recharge and saltwater intrusion in a coastal groundwater system in Vietnam, Hydrogeology Journal, 22, 1749-1762,
818 2014.
819 Tapley, B. D., Bettadpur, S., Ries, J. C., Thompson, P. F., and Watkins, M. M.: GRACE measurements of mass variability in
820 the Earth system, Science, 305, 503-505, 2004.
821 Tiwari, V. M., Wahr, J., and Swenson, S.: Dwindling groundwater resources in northern India, from satellite gravity
822 observations, Geophys. Res. Lett., 36, L18401, 10.1029/2009GL039401, 2009.
823 van der Kamp, G., and Gale, J. E.: Theory of Earth tide and barometric effects in porous formations with compressible
824 grains, Water Resources Research, 19, 538-544, 1983.
825 van der Kamp, G., and Maathuis, H.: Annual fluctuations of groundwater levels as a result of loading by surface moisture,
826 Journal of Hydrology, 127, 137-152, 1991.
827 van der Kamp, G., and Schmidt, R.: Monitoring of total soil moisture on a scale of hectares using groundwater peizometers,
828 Geophysical Research Letters, 24, 719-722, 1997.
829 van der Kamp, G., and Schmidt, R.: Review: Moisture loading - the hidden information in groundwater observation well
830 records, Hydrogeology Journal, 25, 2225-2233, 10.1007/s10040-017-1631-z, 2017.
831 Verruijt, A.: Elastic storage of aquifers, in: Flow through porous media, edited by: Weist, R. J. M. d., Academic Press Inc.,
832 New York, 331-376, 1969.
833 Xu, X., Huang, G., Qu, Z., and Pereira, L. S.: Using MODFLOW and GIS to assess changes in groundwater dynamics in
834 response to water saving measures in irrigation districts of the Upper Yellow River Basin, Water Resources Management,
835 25, 2035-2059, 2011.
836
837